Analyst

Accepted Manuscript

ROYAL SOCIETY OF CHEMISTRY

www.rsc.org/analyst

Cite this: DOI: 10.1039/c0xx00000x

www.rsc.org/xxxxxx

ARTICLE TYPE

Development of a Single Aptamer-based Surface Enhanced Raman Scattering Method for Rapid Detection of Multiple Pesticides

Shintaro Pang,[a] Theodore P. Labuza[b] and Lili He*[a]

Received (in XXX, XXX) Xth XXXXXXXXX 20XX, Accepted Xth XXXXXXXXX 20XX

DOI: 10.1039/b000000x

The objective of this study was to develop a simple and rapid method that could detect and discriminate four specific pesticides (isocarbophos, omethoate, phorate, profenofos) using a single aptamer-based capture procedure followed by Surface Enhanced Raman Spectroscopy (SERS). The aptamer is a single stranded DNA sequence that is specific to capture these four pesticides. The thiolated aptamer was conjugated onto silver (Ag) dendrites, a nanostructure that can enhance the Raman fingerprint of pesticides, through Ag-thiol bonds. It was then backfilled with 6-mercaptohexanol (MH) to prevent nonspecific binding. The modified SERS platform [Ag-(Ap+MH)] was then mixed with each pesticide solution (P) for 20 min. After capturing the pesticides, the Ag-(Ap+MH)-P complex was analyzed under a DXR Raman Microscope and TQ Analyst software. The results show that the four pesticides can be captured and detected using principal component analysis based on their distinct fingerprint Raman peaks. The limits of detection (LODs) of isocarbophos, omethoate, phorate, and profenofos were 3.4 µM (1 ppm), 24 µM (5 ppm), 0.4 µM (0.1 ppm), and 14 µM (5 ppm) respectively. This method was also validated successfully in apple juice. These results demonstrated the super capacity of aptamer-based SERS in rapid detection and discrimination of multi-pesticides. This technique can be extended to detect a wide range of pesticides using specific aptamers.

INTRODUCTION

The development of rapid detection techniques for pesticide residual analysis has become a hot topic in recent years due to increased application of pesticides and fear of its health deteriorating effects.[1,2] This field of analysis is termed "QuEChERS" for finding methods that include making the process to be Quick, Easy, Cheap, Effective, Rugged, and Safe.[3] Traditional/currently-used methods mostly apply chromatography (i.e. GC or LC) coupled with MS.[4–6] Despite its sensitivity and capability to detect multiple residues quantitatively, this method carries several disadvantages including extensive sample preparation (i.e. extraction, filtration, etc.), need for technical expertise and high cost.

Many alternative methods, such as ELISA,[7–9] radioimmunoassay[10,11] and multiarray biosensor methods,[12] have been developed for rapid and sensitive detection of pesticide residues. In these cases, a recognition element captures the target analyte, and in doing so, the receptor-analyte complex produces a biochemical signal (i.e. change in pH, color, radioactivity, charge potential, etc.) that can be qualitatively or quantitatively determined by an appropriate transducer (i.e. signal probe).[13] However, these methods are not without drawbacks. For example, the recognition element might exhibit broad specificity, potentially capturing substrates that are unrelated. The signals produced by the transducer are also often secondary, meaning that the output can only tell us if something was captured. This can be disadvantageous as the analyst will not be sure if the signal came from the target analyte or from some other compound that triggered a similar signal.

Surface-enhanced Raman scattering (SERS) is a powerful spectroscopic technique utilizing nanotechnology and Raman spectroscopy that can detect traces of closely adsorbed molecules on metallic nanostructures (often gold or silver).[14] Even though SERS methods can be conditioned to be sensitive enough to detect a single molecule, SERS alone will not single-handedly separate compounds present in a sample. This might prove to be disadvantageous, especially when detecting trace amounts of a target in a complex matrix like food. In this case, Raman signals from the target analyte will be drowned out by the signal of other ingredients/compounds present, thus making it impossible to detect anything.

To overcome the non-specific nature of SERS, aptamers can be deployed as suitable capture agents. Aptamers are single stranded oligonucleotides that can be synthesized in vitro to capture target molecules. They have become increasingly popular as a capture agent because it is adaptable to various targets, convenient in screening, reproducible for synthesis, versatile in labelling, immobilizing, signalling and regenerating.[15,16] In addition, recent technological advancements have made it faster and cheaper to create new aptamers, particularly through the SELEX (Systemic Evolution of Ligands by Exponential Enrichment) protocol.[17]

Aptamer based SERS method has been previously evaluated on proteins in liquid foods.[18] However, the problem of non-specific binding by other food components has not been solved. The objective of this study was to evaluate the feasibility of an aptamer-based SERS technique for pesticide detection in a complex liquid food (e.g. apple juice) using a single aptamer that was previously synthesized to be specific to

not one, but four commercially available pesticides (isocarbophos, omethoate, profeonofos, phorate).[19] The optimization of aptamer conjugation to eliminate the nonspecific binding in apple juice as well as the feasibility of multi-detection was emphasized and discussed. To the best of our knowledge, very few studies have been published on aptamer-based SERS for small molecule detection.[20,21] No similar study has been reported for detection in a complex food matrix.

EXPERIMENTAL SECTION

Materials

All the chemicals were of analytical reagent grade and were purchased through Fisher Scientific unless otherwise noted. The multiple pesticide binding aptamer (SS2-55) reported previously[19] with the sequence 5'-AAG CTT GCT TTA TAG CCT GCA GCG ATT CTT GAT CGG AAA AGG CTG AGA GCT ACG C-3' with disulfide (S-S) modification at the 5' end was purchased through Eurofins Operon MWG (Ebersberg, Germany). Apple Juice (Stop N Shop, MD, USA) was purchased from a local grocery store.

Preparation of dendritic silver (Ag) nanoparticles

Silver (Ag) dendrites were synthesized in accordance with previously published methods.[22,23] Briefly, a zinc metal plate was rinsed with 1M HCl to remove any metal oxides forming on the outer layer, then rinsed with double distilled water and dried. The zinc plate was then immersed in a 200 mmol $AgNO_3$ (aq) solution for exactly 1 min, which produced nanoparticle size diameters of ≈50 nm. After incubation, the silver dendrites formed on the surface of the zinc plate was gently peeled off and washed with double distilled water several times. SEM images obtained from FEI Magellan 400 (FEI, Oregon, USA) confirmed consistent nanoparticles sizes of ≈50 nm in diameter were crystallized and form a dendritic structure (Fig. 1). This unique structure can provide locally consistent enhancement factor and have been previously demonstrated as a sensitive and reliable SERS substrate. [22,24,25]

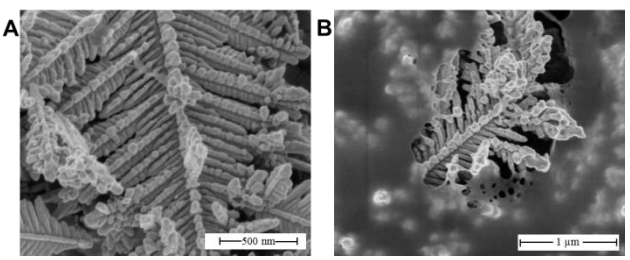

Fig. 1 SEM image of **(A)** silver dendrites and **(B)** thiolated aptamer (S2-55) conjugated onto silver dendrites.

Conjugation of deprotected aptamer onto Ag dendrites

The step by step sequence for developing this single aptamer-based SERS method is illustrated in Fig. 2. Aptamer was first dissolved in a 1xTE buffer (pH 7.4) to give a stock concentration of 129 µM. 100 µl of the aptamer stock solution was then added to 10 mM Tris (2-carboxyethyl) phosphine hydrochloride (TCEP) (i.e. concentration ratio was 1:77) and incubated for 1 hour in order to reduce the disulfide (S-S) to thiol (SH) groups, which has stronger binding affinity to the Ag surface. Then, 30 µl of the aptamer solution was mixed with 370 µl of 1 M phosphate buffer (pH 7), after which 100 µl (≈400 µg) Ag was added. This mixture was homogenized by mixing them together briefly with a micropipette tip. The mixture was then incubated at room temperature for 4 hours on a Nutating mixer (Fisher Scientific) at the speed of 24 rpm to allow the aptamer to conjugate onto the Ag through Ag-thiol binding interaction.

Addition of blocker molecule (i.e. 6-mercaptohexanol) onto silver-aptamer complex (Ag-Ap)

In order to eliminate all forms of non-specific binding interactions with Ag, 40 µM 6-mercaptohexanol (MH) was incubated with Ag-Ap for 1 hour, after which it was rinsed 3 times with double distilled water to fabricate our modified Ag dendrites [Ag-(Ap+MH)].

Detection of multiple specific pesticides using aptamer-based SERS

The pesticides (isocarbophos, omethoate, phorate, profenofos) were spiked in a buffer containing 300 mM NaCl, 50 mM KCl, 10 mM MgCl2, 50 mM Tris/HCl, pH 8.3. 5µl of Ag-(Ap+MH) was added to 400 µl of spiked buffer solution, stirred and incubated for 20 minutes. After incubation, the mixture was centrifuged at 6000 × g for 1 min to allow the modified Ag dendrites and the captured pesticides [Ag-(Ap+MH)-P] to settle to the bottom. The supernatant was then removed and Ag-(Ap+MH)-P was quickly rinsed with double distilled water twice before being deposited onto a glass slide to dry. If testing the pure pesticide solution, this washing and drying step can be minimized. But if the detection is in a complex matrix, i.e. apple juice, a quick wash step is necessary to remove food components.

Raman instrumentation

After drying, the samples were analyzed immediately using a DXR Raman Spectro-microscope (Thermo Scientific, Madison, WI) with the following conditions: 10× confocal microscope objective (3 µm spot diameter and 5 cm−1 spectral resolution), 780 nm excitation wavelength, 5 mW laser power and 50 µm slit width for 2 s integration time. OMNIC™ software version 9.1 was used to control the Raman instrument. Eight spots were selected randomly for each sample within the range of 100-3300cm^{-1}.

Data analysis

SERS spectral data were analyzed using TQ Analyst software (version 8.0) from Thermo Scientific. The SERS spectra obtained from the multiple spots from each sample were averaged and compared against other samples. Second derivative transformation and smoothing were applied at times in order to reduce spectral noise and to separate overlapping bands. The variances of spectral data between spots and samples were then assessed using principal component analysis (PCA). This method focuses a multidimensional data set to the most dominant features while removing random variation so that the principal components can be used to capture the variation between spectra. This discriminant analysis is thus useful in evaluating SERS spectra for variance within a class and between classes. Generally speaking, if two data clusters (classes) do not overlap, then it means they are significantly different at the $p = 0.05$ level. The limit of detection LOD was determined to be the lowest concentration of the data cluster that can be separated from the negative control in the PCA plot. Partial least square (PLS), a multivariate analysis model, was also applied to see if there was a linear relationship between the obtained spectral peak intensities and the actual spiked concentrations.

RESULTS AND DISCUSSIONS

Optimization of aptamer conjugation with Ag

In order to maximize Ag-Ap conjugation, various concentrations of aptamers up to 0.512 µM were initially added to 100 µl Ag in

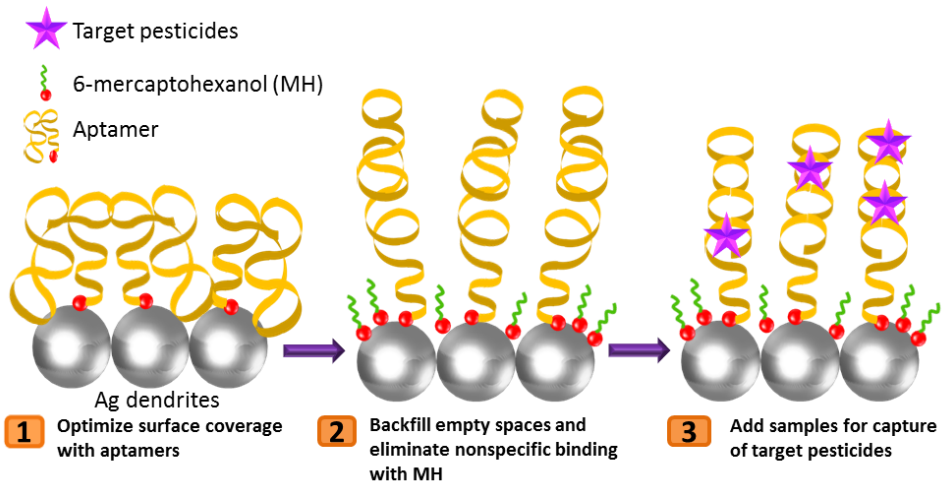

Fig. 2 The schematic illustration of the development of the single aptamer-based SERS method for the detection of four specific pesticides (isocarbophos, omethoate, phorate, profenofos).

water as the solvent. The SERS spectra were then analyzed to pick out the concentration with the highest aptamer peak (i.e. highest amount of aptamers bound to Ag).[26] Interestingly, the aptamer peak intensities started to decrease after 0.128 µM (Fig. S1). This could be explained due to the intermolecular electrostatic repulsion from the negatively charged ssDNA molecules. In order to minimize the intermolecular electrostatic repulsion, 1 M phosphate buffer (pH 7) was used as a medium to increase the ionic strength, thus electrostatically shielding the charged oligonucleotides.[27] This caused the aptamer peak intensities to increase significantly at higher aptamer concentrations up to 5 µM (Fig. 3), thus proving the need for a higher level of salts to increase surface coverage. Other medium such as Tris buffers, chloride and nitrate salts were also tested to evaluate their effectiveness in increasing aptamer optimization, but they brought other problems (i.e. clumping/reaction of Ag nanoparticles), and subsequent reduction in SERS peak intensities. Incubation time to optimize aptamer surface coverage was also evaluated (up to 24 hours) and it was found that after 4 hours, the coverage was optimized (Fig. S2). This result was consistent with other findings that showed thiol-derivative oligonucleotide having optimized surface coverage after 4 hours.[27,28]

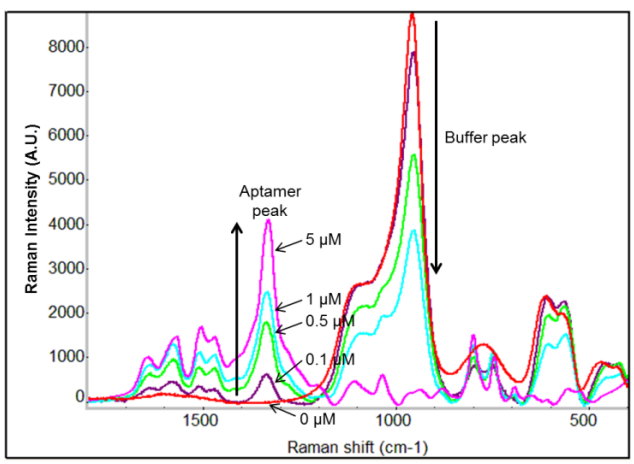

Fig. 3 Raman spectra showing the concentration optimization of thiolated aptamer (S2-55) on 100 µl Ag dendrites in 1M phosphate buffer, pH 7. As the thiolated aptamer concentration increased, the aptamer peaks, notably around 1330 cm^{-1}, increased up to 5 µM. At the same time, the Raman intensities of other competing molecules in the buffer decreased. At 5 µM, the buffer peak 970 cm^{-1} is no longer reflected on the Raman spectra, suggesting complete displacement by the thiolated aptamer.

Optimization of MH concentration and incubation time with Ag-Ap

Since aptamers are relatively large molecules, maximizing its surface coverage on Ag does not ensure elimination of non-specific binding to Ag because steric hindrance can occur. The small, empty spaces between the aptamers can become non-specific binding sites for smaller molecules (e.g. pesticides, salts, food matrix). Furthermore, although Ag can bind specifically to thiolated aptamers through Ag-thiol bonds, Ag will also interact non-specifically with the N1 groups present on the A, T, G, C ring functional groups of the aptamer.[27,29] This particular interaction will likely make them incapable of capturing their target agents since their 3D conformation will be unable to change.

In order to eliminate non-specific binding and to ensure that the aptamer is free to change its 3D conformation during target capture, a small blocker molecule (i.e. 6-mercaptohexanol) was introduced.[30] Since this molecule is relatively very small, it does not interfere with the 3D conformational change that occurs when the aptamer is capturing its target. In addition, its thiol end has a strong binding affinity to Ag, thus enabling displacement of any non-specific binding of aptamers or other molecules (e.g. TCEP) that might be present in the Ag-Ap complex. Inadvertently, studies have shown that high concentrations and longer incubation times of MH can even displace thiolated oligonucleotides,[30,31] thus it was essential to optimize the time/concentration of added MH to fully cover the empty surface area and to displace non-specific binding, but at the same time, to minimize displacement of the thiolated aptamer. Varying concentrations (0-1 mM) of MH and varying incubation times (0-1 h) were tested and their Raman spectra were analyzed to monitor the appearance of MH peaks and aptamer peak intensities. As the MH concentration and incubation time

increased, the Raman peaks attributed to MH increased, but at the same time, the peaks attributed to the aptamer decreased, albeit at a lower extent. The optimized time/concentration was determined to be 40 µM for 1 h because the Raman peaks from MH were visible while the aptamer peak intensities did not drop drastically (Fig. 4). This observation was in line with another study that showed that when MH was introduced to thiolated oligonucleotides conjugated to gold nanoparticles, the oligonucleotides started to become displaced after using 10 µM of MH for 10 mins and a significant displacement was observed when 100 µM MH was incubated for 10 mins.[30]

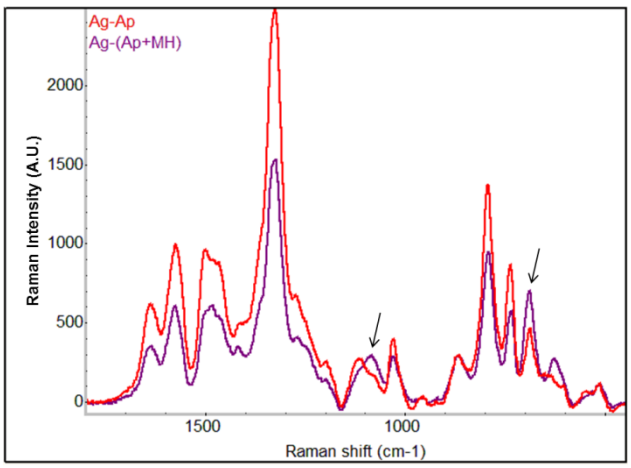

Fig. 4 Raman spectra of Ag-Ap and Ag-(Ap+MH). 40 µM MCH was incubated for 1 h with Ag-Ap and analyzed to produce the Raman spectra for Ag-(Ap+MH). The Raman peaks at 680 and 1080 cm^{-1} are both attributed to the capture of MH. The decrease in aptamer peaks (e.g. 1330 cm^{-1}) is inevitable due to the strong binding dissociation nature of MH.

One visual test to see if the nanoparticles had been fully covered with the aptamer and MH was by adding it into the capture buffer solution. When bare Ag dendrites were added to the buffer, they aggregated immediately. When Ag-Ap was added to the buffer, it remained dispersed for a few minutes, but slowly started to aggregate as time went on. However, when the fully modified Ag dendrites [Ag-(Ap+MH)] was added to the buffer, it remained dispersed for as long as 20 min without any aggregation, thus proving that the Ag dendrites had been fully covered by the aptamer and MH (data not shown).

Detection of multiple pesticides using Ag-(Ap+MH)

The chemical structures of the four target pesticides are shown in Fig. 5A.

Pesticides at varying concentrations (0-0.5 mM) individually or as a mixture were initially spiked in water before Ag-(Ap+MH) was added. However, when the Raman spectra were measured, there was no noticeable capture of any of the pesticides. Furthermore, among the 8 replicates tested for each sample, the aptamer peaks were very inconsistent (data not shown). This could be due to the instability of the aptamers in a medium that does not have cations, as they are being introduced in the buffers used to select the aptamers.[19] In addition, some other aptamer papers have reported the dependency of cations to form stable 3D conformations to ensure the capture of their target agents.[32,33] Therefore, the aptamer selection buffer was then employed as a capture buffer.

Raman spectra show a huge difference in pesticide capture peaks when the capture buffer was used. As shown in Fig. 5B, each pesticide capture produces distinct peaks at different Raman shifts, signifying the capture of the target pesticides. Fig. 5B highlights the most noticeable difference between each pesticide and the control. Their full spectra are shown in the supporting information (Fig. S3).

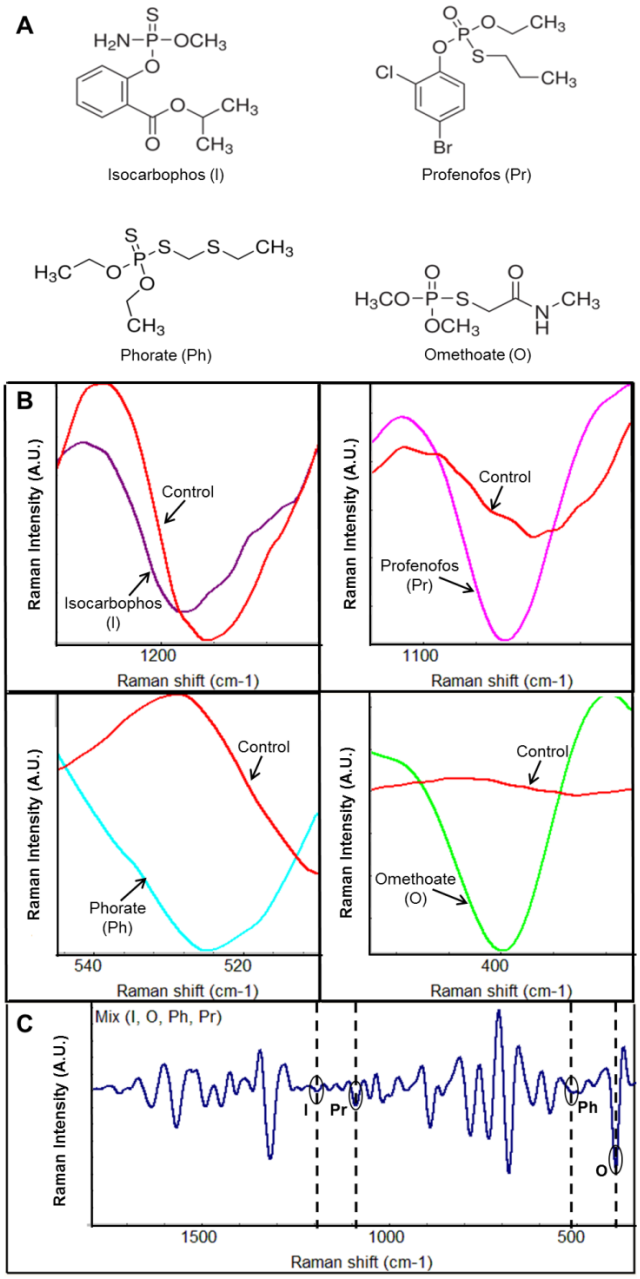

Fig. 5 (A) Chemical structure of the four pesticides that is specific to the aptamer being used. **(B)** Second derivative transformation of the Raman spectra of an isocarbophos capture peak and the control between 1220-1170 cm^{-1}; a profenofos capture peak and the control between 1110-1060 cm^{-1}; a phorate capture peak and the control between 545-510 cm^{-1}; an omethoate capture peak and the control between 425-375 cm^{-1}. The control was the modified Ag dendrites [Ag-(Ap+MH)]. The spiked concentration for the four pesticides was 0.5 mM. All samples were conducted in a capture buffer with a 20 min incubation period. The raw spectra yielded similar trends (Fig. S4). **(C)** A second derivative Raman spectra reflecting the capture of all four pesticides (isocarbophos,

profenofos, phorate, omethoate) by Ag-(Ap+MH). 125 µM of each pesticide was added. Distinct Raman peaks were produced at different Raman shifts that correlated with each individual pesticide capture peak.

Because each pesticide produces distinct Raman peaks, the type of pesticides being captured can be discriminated based on the peak intensities at various Raman shifts. Furthermore, by looking at the principal component analysis score, the whole spectrum can be analyzed to see if these peaks are significantly different from each other. In this case, all four pesticides that are specific to this aptamer produced significantly different Raman spectra peaks from each other and the control (i.e. no pesticide) (Fig. 6). This shows that the Raman peak changes attributed to the pesticides can be statistically quantified and differentiated. The four pesticides were also added together as a mixture and measured to find out if they could all be detected at the same time (Fig. 5C). By looking at each distinct Raman peak from each pesticide capture, it was found to be correlated with a Raman peak that appeared in the mixture. Thus, this method provides a method that can identify four specific pesticides with one sample. On the other hand, when acetamiprid, a pesticide not specific to this apatamer was introduced, no visible pesticide capture peaks were seen (data not shown), thus validating the aptamer's high specificity.[19] The great advantage of this technique is not only that it can measure multiple target analytes, but it can also simultaneously validate that the captured molecules are the target analytes based on their specific signature peaks at certain Raman peak shifts. This unique "self-validation" method ensures great accuracy of this technique, superior to other sensor techniques that are based on color, fluorescence or electrochemical signals and begins to satisfy many of the requirements of "QuChERS".

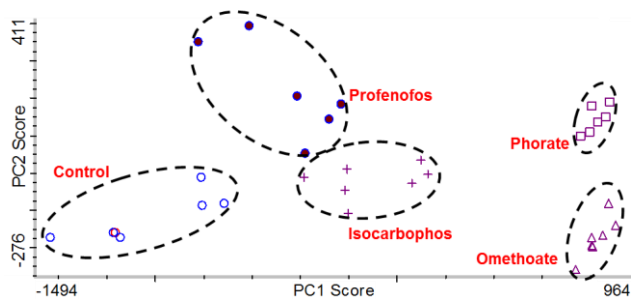

Fig. 6 PCA plot comparing the second derivative Raman spectra of each pesticide (0.5 mM) captured by modified Ag dendrites [Ag-(Ap+MH)] as well as the control. This result shows significant differences between each pesticide capture, proving the detection and discrimination of the four pesticides.

Determination of the limit of detection and quantitative capability of this method

Fig. 7A shows the relationship between the phorate capture peaks and the phorate concentration. The limit of detection (LOD) was determined to be 0.4 µM (0.1 ppm) by PCA (Fig. 7B). The LODs of other pesticides were also determined and are shown in Fig. S5. Compared with the LOD of phorate, the LODs of iscocarbophos (3.5 µM = 1 ppm), omethoate (24 µM = 5 ppm) and profenofos (14 µM = 5 ppm) were much higher, although the reported binding dissociation constants were similar for these four pesticides. One hypothesis is that the phorate molecules after being captured by the aptamers were positioned in a distance closer to the surface of Ag-(Ap+MH) compared with other molecules or the interaction between phorate and aptamer resulted in a specific charge transfer mechanism that enhanced the Raman scattering of phorate. More studies are needed to understand this phenomenon. The LOD of pesticides obtained from this method was also compared with currently used methods[4–6] (i.e. chromatography). The sensitivity of this SERS method was found to be slightly lower. Nevertheless, the LODs mainly depend on the binding dissociation constants of the aptamer. Aptamers that are specific to smaller molecules tend to have a lower binding affinity due to the limited binding sites available for the aptamer to bind to the molecule.[34] Thus, this method can be further improved by selecting and applying an aptamer of higher binding dissociation constants.

The quantitative capability of this method to phorate was also evaluated. The partial least square line depicting the relationship between the calculated phorate concentration based on the phorate capture peak and the actual spiked phorate concentration added shows a linear relationship within the range of 0-3.8 µM (10 ppm) with a root mean square error coefficient of 0.9628 (Fig. S6). However, not all pesticides had such a linear response. It was found, at high concentrations (i.e. 0.5 mM), the captured omethoate produced the most profound peak intensities among the four pesticides. However, at lower concentrations (i.e. 4.8-48 µM), the captured omethoate produced little enhanced peaks compared to the other pesticides, suggesting that Raman peak intensities are not linearly correlated with omethoate concentration. Little is known about this relationship and more studies will be needed to understand the molecular mechanism behind this phenomenon.

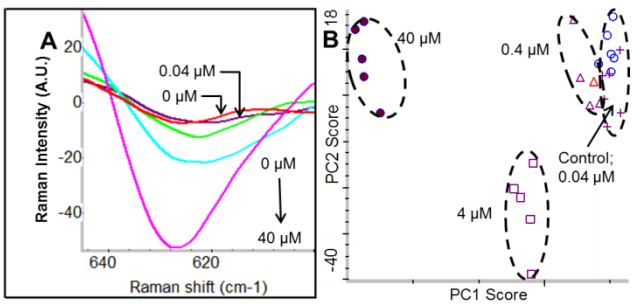

Fig. 7 (A) Second derivative Raman spectra of the phorate capture peak between 645-600 cm^{-1} when 0, 0.04 µM, 0.4 µM, 4 µM and 40 µM phorate were exposed to the modified Ag dendrites [Ag-(Ap+MH)]. This result shows an increase in peak intensity around 625 cm^{-1} as phorate concentration increases; **(B)** PCA plot for Raman spectra of phorate at 0 µM-Control (○), 0.04 µM (+), 0.4 µM (△) , 4 µM (□) and 40 µM (●). A significant difference was seen beginning at 0.4 µM.

Method validation in apple juice to ensure elimination of non-specific binding and applicability in food matrix

When Ag was exposed to liquid foods (e.g. apple juice), nonspecific binding interaction occurred rampantly, causing multiple Raman peaks to form that easily drowned the target agent peaks. In order to validate the elimination of non-specific binding, the prepared complex [Ag-(Ap+MH)] was incubated with apple juice by adding 100 µL of apple juice into 900 µL of optimized Ag complex in buffer. The spectrum in apple juice showed no significant changes in peaks compared with the one in buffer (Fig. 8A), proving that non-specific binding was eliminated. When phorate was added to apple juice, phorate

intense capture peaks appeared, signifying the capture of phorate in apple juice. Analysis of the other pesticides spiked with apple juice was also performed and the results showed similar trends as phorate (Fig. S7). Furthermore, a mixture of all four pesticides yielded results similar to the same experiment done without apple juice (Fig. 8B), although the sensitivity for each pesticide was different. This may be due to a change in incubation environment (i.e. pH, presence of other solutes) that deterred from the optimized condition. It is therefore worthy to note that an optimized dilution of the apple juice was needed to produce the most intense phorate capture peaks. At higher apple juice concentrations, the food components might alter the optimized condition for the Ag complex to function. Nevertheless, this method can be easily applied to other food and beverage samples for more effective capture and analysis.

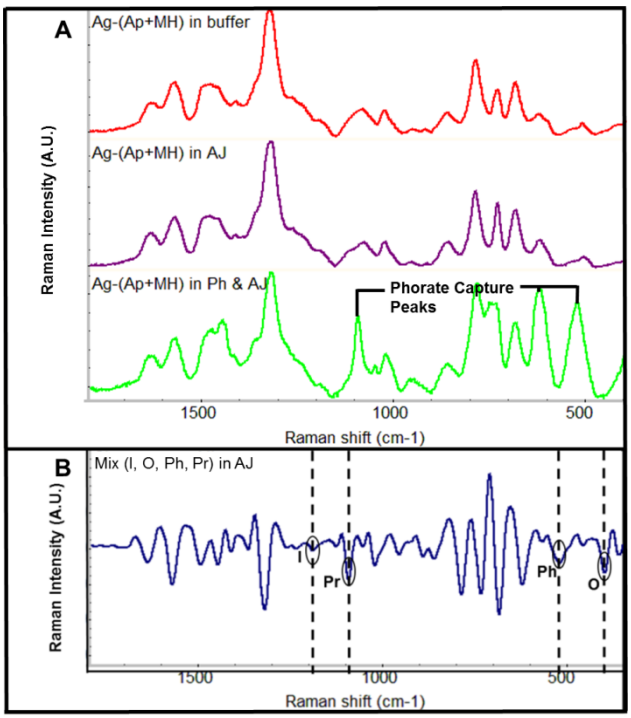

Fig. 8 (A) Raman spectra of modified Ag dendrites [Ag-(Ap+MH)] mixed with (from top to bottom) capture buffer, apple juice (diluted 1:10) (AJ), and phorate (Ph) (0.5 mM) spiked in AJ. Spectral results show no differences between Ag-(Ap+MH) exposed to buffer and AJ, suggesting nonspecific binding has been eliminated. However, when Ag-(Ap+MH) was exposed to Ph & AJ, huge spectral change was observed, proving the capture of phorate. **(B)** A second derivative Raman spectra reflecting the capture of all four pesticides (isocarbophos, profenofos, phorate, omethoate) by Ag-(Ap+MH) in AJ. The obtained results were similar to the experiments done without AJ (Fig. 5C).

CONCLUSIONS

In summary, a single aptamer based SERS method for detecting multiple specific pesticides in complex liquid food (i.e. apple juice) was established. The elimination of nonspecific binding was achieved by optimization of aptamer conjugation and with the blocker molecule MH to fill the empty spaces. The detection, discrimination, and validation of multiple pesticides using aptamer-based SERS method were achieved based on their distinct Raman fingerprint peaks. Furthermore, simultaneous detection of multiple pesticides was shown using the SERS spectra obtained. Total analytical time for measuring six samples was 40 min. The developed aptamer SERS method shows great potential to analyze pesticide residues in apple juice. Further experiment is needed to explore the application in other food matrices.

ACKNOWLEDGMENTS

This project was supported by the Agriculture and Food Research Initiative Program of the US Department of Agriculture (USDA-AFRI, grant No.: 2012-67017-30194).

Notes and references

[a] *Department of Food Science, University of Massachusetts, Amherst, MA , USA. Tel: (413)545 5847; E-mail:lilihe@foodsci.umass.edu*
[b] *Department of Food Science and Nutrition, University of Minnesota, St. Paul, MN 55108, USA.*

† Electronic Supplementary Information (ESI) available: [Supporting figures that details some of the secondary steps that were taken into account in order to develop the single aptamer based SERS method for detecting multiple pesticides. Fig. S1-S7]. See DOI: 10.1039/b000000x/

‡ Footnotes should appear here. These might include comments relevant to but not central to the matter under discussion, limited experimental and spectral data, and crystallographic data.

1. B. Jin, L. Xie, Y. Guo, and G. Pang, *Food Res. Int.*, 2012, **46**, 399–409.
2. D. Liu, W. Chen, J. Wei, X. Li, Z. Wang, and X. Jiang, *Anal. Chem.*, 2012, **84**, 4185–91.
3. M. Anastassiades, S. Lehotay, and D. Štajnbaher, in *18th Annual waste testing and quality symposium proceeding*, Arlington, VA, 2002, pp. 231–241.
4. J. Lee and H. K. Lee, *Anal. Chem.*, 2011, **83**, 6856–61.
5. M. a Martínez-Uroz, M. Mezcua, N. Belmonte Valles, and a R. Fernández-Alba, *Anal. Bioanal. Chem.*, 2012, **402**, 1365–72.
6. J. S. Punzi, M. Lamont, D. Haynes, and R. L. Epstein, *Outlooks Pest Manag.*, 2005, **16**, 131–137.
7. L. Wang, Q. Zhang, D. Chen, Y. Liu, C. Li, B. Hu, D. Du, and F. Liu, *Anal. Lett.*, 2011, **44**, 1591–1601.
8. Z.-L. Xu, H. Deng, X.-F. Deng, J.-Y. Yang, Y.-M. Jiang, D.-P. Zeng, F. Huang, Y.-D. Shen, H.-T. Lei, H. Wang, and Y.-M. Sun, *Food Chem.*, 2012, **131**, 1569–1576.
9. X. Hua, L. Wang, G. Li, Q. Fang, M. Wang, and F. Liu, *Anal. Methods*, 2013, **5**, 1556.
10. C. D. Ercegovich, R. P. Vallejo, R. R. Gettig, L. Woods, E. R. Bogus, and R. O. Mumma, *J. Agric. Food Chem.*, 1981, **29**, 559–63.
11. J. C. Hall, R. J. A. Deschamps, and K. K. Krieg, *J. Agric. Food Chem.*, 1989, **37**, 981–984.
12. Y. Guo, J. Tian, C. Liang, G. Zhu, and W. Gui, *Microchim. Acta*, 2013, **180**, 387–395.
13. S. White, in *Handbook of Food Analysis, Second Edition -3 Volume Set*, ed. L. Nollet, CRC Press, 2004, pp. 2133–2148.
14. H. Im, K. C. Bantz, N. C. Lindquist, C. L. Haynes, and S.-H. Oh, *Nano Lett.*, 2010, **10**, 2231–6.
15. J.-W. Chen, X.-P. Liu, K.-J. Feng, Y. Liang, J.-H. Jiang, G.-L. Shen, and R.-Q. Yu, *Biosens. Bioelectron.*, 2008, **24**, 66–71.
16. Y. Dong, Y. Xu, W. Yong, X. Chu, and D. Wang, *Crit. Rev. Food Sci. Nutr.*, 2013, 130524060823006.
17. A. D. Ellington and J. W. Szostak, *Nature*, 1992, **355**, 850–2.
18. L. He, E. Lamont, B. Veeregowda, S. Sreevatsan, C. L. Haynes, F. Diez-Gonzalez, and T. P. Labuza, *Chem. Sci.*, 2011, **2**, 1579.
19. L. Wang, X. Liu, Q. Zhang, C. Zhang, Y. Liu, K. Tu, and J. Tu, *Biotechnol. Lett.*, 2012, **34**, 869–74.
20. M. Li, J. Zhang, S. Suri, L. J. Sooter, D. Ma, and N. Wu, *Anal. Chem.*, 2012, **84**, 2837–42.
21. F. Barahona, C. L. Bardliving, A. Phifer, J. G. Bruno, and C. a. Batt, *Ind. Biotechnol.*, 2013, **9**, 42–50.
22. L. He, M. Lin, H. Li, and N.-J. Kim, *J. Raman Spectrosc.*, 2010, **41**, 739–744.

23. B. D. J. Fang, H. You, P. Kong, Y. Yi, X. Song, *Cryst. Growth Des.*, 2007, **7**, 864–867.
24. L. He, T. Rodda, C. L. Haynes, T. Deschaines, T. Strother, F. Diez-Gonzalez, and T. P. Labuza, *Anal. Chem.*, 2011, **83**, 1510–3.
25. K. G. M. Laurier, M. Poets, F. Vermoortele, G. De Cremer, J. A. Martens, H. UjI-i, D. E. De Vos, J. Hofkens, and M. B. J. Roeffaers, *Chem. Commun. (Camb).*, 2012, **48**, 1559–61.
26. L. He, B. D Deen, A. H. Pagel, F. Diez-Gonzalez, and T. P. Labuza, *Analyst*, 2013, **138**, 1657–9.
27. T. M. Herne and M. J. Tarlov, *J. Am. Chem. Soc.*, 1997, **119**, 8916–8920.
28. K. A. Peterlinz, R. M. Georgiadis, T. M. Herne, and M. J. Tarlov, *J. Am. Chem. Soc.*, 1997, **119**, 3401–3402.
29. P. Sandstrom, M. Boncheva, and B. Akerman, *Langmuir*, 2003, **19**, 7537–7543.
30. S. Park, K. a. Brown, and K. Hamad-Schifferli, *Nano Lett.*, 2004, **4**, 1925–1929.
31. A. Wijaya, S. B. Schaffer, I. G. Pallares, and K. Hamad-Schifferli, *ACS Nano*, 2009, **3**, 80–86.
32. P. Jayapal, G. Mayer, A. Heckel, and F. Wennmohs, *J. Struct. Biol.*, 2009, **166**, 241–50.
33. W. S. Ross and C. C. Hardin, *J. Am. Chem. Soc.*, 1994, **116**, 6070–6080.
34. M. McKeague and M. C. Derosa, *J. Nucleic Acids*, 2012, **2012**, 748913.

Graphical Abstract

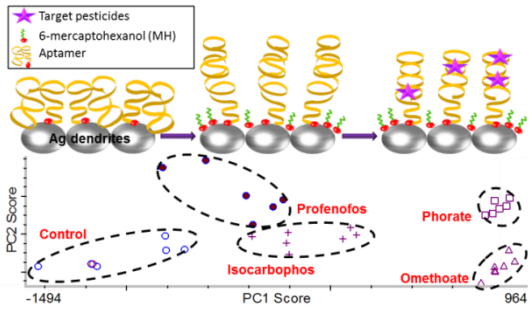

A single aptamer-based SERS method is developed for the detection and discrimination of four specific pesticides (isocarbophos, omethoate, phorate, profenofos).